

A Study on Optimization of Waveguide Dispersion Property Using Function Expansion Based Topology Optimization Method

Hiroyuki GOTO^{†a)}, Student Member, Yasuhide TSUJI^{†b)}, Takashi YASUI^{††c)},
and Koichi HIRAYAMA^{††d)}, Members

SUMMARY In this paper, the function expansion based topology optimization is employed to the automatic optimization of the waveguide dispersion property, and the optimum design of low-dispersion slow-light photonic crystal waveguides is demonstrated. In order to realize low-dispersion and large group index, an objective function to be optimized is expressed by the weighted sum of the objective functions for the desired group index and the low-dispersion property, and weighting coefficients are updated through the optimization process.

Key words: function expansion method, topology optimization, photonic crystal waveguide, slow-light, structural filter

1. INTRODUCTION

In the rapid spread of the Internet, the demand for high speed and large capacity photonic network has been increasing and the developments of novel high performance photonic circuit devices are required. In order to develop high performance photonic devices, now, computer simulations are widely used and automatic optimization techniques using them are also proposed. Among them, the topology optimization is a powerful optimization method which can optimize topological configuration and it has already been applied to several optimization problems of photonic circuit devices [1]–[10].

In the standard topology optimization based on the density method [1], [2], [4]–[9], the density parameters are continuous and can be an intermediate value between 0 and 1. This corresponds to an intermediate value between the refractive indices of usable materials (gray area). On the other hand, the function expansion based topology optimization can easily suppress the gray area and its usefulness has been demonstrated in the transmission problems [3], [10].

In this paper, the function expansion based topology optimization is employed to optimize the waveguide dispersion property and the automatic optimum design of low-dispersion slow-light photonic crystal waveguides (PCWGs) [11] is demonstrated. In order to realize low-dispersion and large group index, an objective function to be

optimized is expressed by the weighted sum of the objective functions for the desired group index and low-dispersion property. In the problems to realize group index of 50 and 100, using standard function expansion method, the optimized PCWGs which have the group index of 50 with the low-dispersion bandwidth of 10.5 nm and the group index of 103 with the low-dispersion bandwidth of 4.3 nm are realized. However, the PCWGs obtained with this optimization and the optimization of the previous studies [10] have a complicated structure. In order to suppress fine structures, we have introduced a structural filter in the optimization process and obtained the simplified structure with almost the same propagation properties.

In section 2, the finite element method (FEM) for periodic waveguides is described briefly. In section 3, we present the formulation for the function expansion based topology optimization. In section 4, design examples are demonstrated. In section 5, we confirm the low dispersion property. In section 6, we introduce a structural filter to suppress the complicated structures and this paper is concluded in section 7.

2. FINITE ELEMENT METHOD FOR PERIODIC WAVEGUIDES

We consider a two-dimensional periodic waveguide, as shown in Fig. 1, in which the structure is periodic in the longitudinal direction (x -direction) with period a and there is no variation along the z -direction ($\frac{\partial}{\partial z} = 0$). From Maxwell's equations, we obtain the following wave equation:

$$\frac{\partial}{\partial x} \left(p \frac{\partial \Phi}{\partial x} \right) + \frac{\partial}{\partial y} \left(p \frac{\partial \Phi}{\partial y} \right) + k_0^2 q \Phi = 0 \quad (1)$$

$$p = 1, q = \epsilon_r, \Phi = E_z \quad \text{for TE mode}$$

$$p = 1/\epsilon_r, q = 1, \Phi = H_z \quad \text{for TM mode}$$

where k_0 is the free space wave number, $\epsilon_r = n^2$ is the relative permittivity (n is the refractive index), E_z and H_z are the z components of the electric and magnetic fields, respectively. Since the field distribution has the same periodicity as the structure, FEM is applied to the region of one period along the x -direction, and the periodic boundary condition is imposed on Γ_1 and Γ_2 . Assuming the steady state propagation with the propagation constant of β , the fields Φ within each element can be approximated as

$$\Phi_e(x, y) = \exp(-j\beta x) \{N\}^T \{\phi\}_e \quad (2)$$

Manuscript received October 19, 2013.

Manuscript revised January 27, 2014.

[†]Information and Electronic Eng., Muroran Institute of Technology

^{††}Electrical and Electronic Eng., Kitami Institute of Technology

a) E-mail: s2024041@gmail.com

b) E-mail: y-tsuji@mmm.muroran-it.ac.jp

c) E-mail: yasui@mail.kitami-it.ac.jp

d) E-mail: hirakc@mail.kitami-it.ac.jp

DOI: 10.1587/transle.E97.C.670

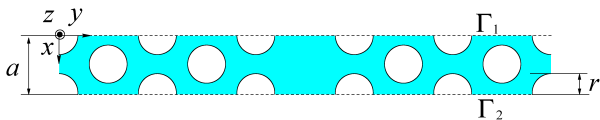


Fig. 1 Analysis region of a photonic crystal waveguide.

where $\{N\}$ is the shape function vector for the quadratic triangular element, $\{\phi\}_e$ is the nodal ϕ vector for each element, and ϕ is the envelope function of Φ . Applying the Galerkin procedure and periodic boundary condition, the following matrix eigenvalue problem, whose eigenvalue is k_0^2 , can be obtained [12].

$$([K(\beta)] - k_0^2[M])\{\phi\} = \{0\} \quad (3)$$

where

$$[K] = \sum_e \iint_e p \left\{ \left(\frac{\partial\{N\}}{\partial x} + j\beta\{N\} \right) \times \left(\frac{\partial\{N\}^T}{\partial x} - j\beta\{N\}^T \right) + \frac{\partial\{N\}}{\partial y} \frac{\partial\{N\}^T}{\partial y} \right\} dx dy \quad (4)$$

$$[M] = \sum_e \iint_e q \{N\} \{N\}^T dx dy \quad (5)$$

We can obtain the eigenvalue k_0^2 and eigenvector $\{\phi\}$ from (3) with the parameter β , and the dispersion property can be also obtained by varying β .

3. FUNCTION EXPANSION BASED TOPOLOGY OPTIMIZATION

3.1 Expression for Permittivity Distribution

Now, if the device is designed using only two kinds of materials, relative permittivity can be defined as follows by using some analytical function $w(x, y)$:

$$\varepsilon_r(x, y) = \varepsilon_{ra} + (\varepsilon_{rb} - \varepsilon_{ra})H(w(x, y)) \quad (6)$$

where ε_{ra} and ε_{rb} are the relative permittivities of the two considered materials. The function $H(\xi)$ takes the value of 0 or 1 depending on the ξ and $\varepsilon_r(x, y)$ at any points is the relative permittivity of either ε_{ra} or ε_{rb} depending on the value of $w(x, y)$. In order to make it possible to take the differential of $H(w(x, y))$ in the sensitivity analysis described in the following subsection, we define $H(\xi)$ as follows:

$$H(\xi) = \begin{cases} 0 & (\xi \leq -h) \\ \frac{1}{2} \left(\frac{\xi+h}{h} \right)^2 & (-h < \xi < 0) \\ 1 - \frac{1}{2} \left(\frac{\xi-h}{h} \right)^2 & (0 \leq \xi < h) \\ 1 & (\xi \geq h) \end{cases} \quad (7)$$

where h has a non-zero value during the optimization process and the relative permittivity takes an intermediate value in $-h < w(x, y) < h$. However, gray area can be removed by setting h to be 0 after the optimization process. In general, $w(x, y)$ is expressed in the form of the superposition of some

analytical function $f_i(x, y)$ as

$$w(x, y) = \sum_i c_i f_i(x, y) \quad (8)$$

By optimizing the value of the coefficient c_i based on the sensitivity analysis, the optimal structure can be obtained. Several kinds of functions can be used for $f_i(x, y)$. In this paper, Fourier series represented by the following equation has been used [3]:

$$w(x, y) = \sum_{i=0}^{N_x-1} \sum_{j=-N_y}^{N_y-1} (a_{ij} \cos \theta_{ij} + b_{ij} \sin \theta_{ij}) \quad (9)$$

$$\theta_{ij} = \frac{2\pi i}{L_x} x + \frac{2\pi j}{L_y} y \quad (10)$$

where N_x and N_y denote the number of expansion terms in the x and y directions, respectively. In this paper, N_x and N_y are set to be 16 and 128, respectively. In order to introduce the periodic structure in the design region, L_x and L_y are set to be the design region width along the x and y directions, respectively.

3.2 Sensitivity Analysis

In the present automatic optimization process, we need to know the dependence of the wavenumber k_0 on the expansion coefficient c_i in (8). Now, we consider the following expression of the relative permittivity with M parameters, c_i ($i = 1, 2, \dots, M$):

$$\varepsilon_r = \varepsilon_r(c_1, c_2, \dots, c_M) \quad (11)$$

According to the matrix eigenvalue equation (3), the eigenvalue k_0^2 is expressed by the eigen field as follow:

$$k_0^2 = \frac{\{\phi\}^\dagger [K] \{\phi\}}{\{\phi\}^\dagger [M] \{\phi\}} \quad (12)$$

where \dagger denotes a complex conjugate transpose. Assuming the field variation by the perturbation of permittivity distribution to be negligible, the sensitivity of k_0 to c_i can be expressed as follows:

$$\frac{\partial k_0}{\partial c_i} = \frac{\{\phi\}^\dagger \frac{\partial [K]}{\partial c_i} \{\phi\}}{2\{\phi\}^\dagger [K] \{\phi\}} - \frac{\{\phi\}^\dagger \frac{\partial [M]}{\partial c_i} \{\phi\}}{2\{\phi\}^\dagger [M] \{\phi\}} \quad (13)$$

where $\frac{\partial [K]}{\partial c_i}$, $\frac{\partial [M]}{\partial c_i}$ in (13) is given by

$$\frac{\partial [K]}{\partial c_i} = 0 \quad (14)$$

$$\frac{\partial [M]}{\partial c_i} = \sum_e \iint_e \frac{\partial \varepsilon_r}{\partial c_i} \{N\} \{N\}^T dx dy \quad (15)$$

for TE modes, and

$$\frac{\partial [K]}{\partial c_i} = - \sum_e \iint_e \frac{\partial \varepsilon_r}{\partial c_i} \frac{1}{\varepsilon_r^2} \left\{ \left(\frac{\partial\{N\}}{\partial x} + j\beta\{N\} \right) \times \left(\frac{\partial\{N\}^T}{\partial x} - j\beta\{N\}^T \right) + \frac{\partial\{N\}}{\partial y} \frac{\partial\{N\}^T}{\partial y} \right\} dx dy \quad (16)$$

$$\frac{\partial[M]}{\partial c_i} = 0 \quad (17)$$

for TM modes. Considering (6), $\frac{\partial \varepsilon_r}{\partial c_i}$ in (15) and (16) is given by

$$\frac{\partial \varepsilon_r}{\partial c_i} = (\varepsilon_{rb} - \varepsilon_{ra}) \frac{\partial w(x, y)}{\partial c_i} \frac{\partial H(w(x, y))}{\partial w(x, y)} \quad (18)$$

3.3 Objective Function

An objective function to be optimized needs to be appropriately set up according to a problem. In this paper, in order to design low-dispersion slow-light PCWGs [4]–[11], the following objective function C is considered.

$$\begin{aligned} \text{Minimize } C = & \int_{\beta_a}^{\beta_b} W_1 \left| \frac{\partial k_0(\beta)}{\partial \beta} - \frac{v_g}{c} \right| d\beta \\ & + \int_{\beta_a}^{\beta_b} W_2 \left| \frac{\partial^2 k_0(\beta)}{\partial \beta^2} \right| d\beta \end{aligned} \quad (19)$$

where v_g is the desired group velocity, β_a and β_b ($\beta_a < \beta_b$) express the design region of the propagation constant. In the actual implementation, (19) is discretized in β and is expressed by

$$\text{Minimize } C = W_1 C^{(1)} + W_2 C^{(2)} \quad (20)$$

$$C^{(1)} = \sum_{i=1}^N |k_0(\beta_i) - \bar{k}_0(\beta_i)| \quad (21)$$

$$C^{(2)} = \sum_{i=2}^{N-1} |k_0(\beta_{i+1}) - 2k_0(\beta_i) + k_0(\beta_{i-1})| \quad (22)$$

where $\beta_1 = \beta_a$, $\beta_N = \beta_b$, $\Delta\beta = \frac{\beta_N - \beta_1}{N-1}$, $W_2 = \frac{w}{\Delta\beta}$, and $\bar{k}_0(\beta_i) = (v_g/c)(i-1)\Delta\beta + k_0(\beta_1)$ is the desired wavenumber for β_i . Minimization of $C^{(1)}$ and $C^{(2)}$ corresponds to realizing the desired group velocity and reducing the wavelength dispersion, respectively. W_1 and W_2 are the parameters which determine the priority of $C^{(1)}$ and $C^{(2)}$. In this paper, the following setting is used:

$$\frac{W_1}{W_2} = \left| \frac{C^{(1)}}{C^{(2)}} \right|, \quad W_1 + W_2 = 1 \quad (23)$$

Using (23), we expect the worse term to be optimized more.

3.4 Update of Permittivity Distribution

In order to obtain the optimum structure, we iteratively update the parameter c_i according to the sensitivity of the objective function C . In this paper, the standard maximum gradient method is employed and each parameter is updated as follows:

$$c'_i = c_i - \frac{1}{|\nabla_c C|} \frac{\partial C}{\partial c_i} \times \delta \quad (24)$$

$$|\nabla_c C| = \sqrt{\sum_{i=1}^M \left| \frac{\partial C}{\partial c_i} \right|^2} \quad (25)$$

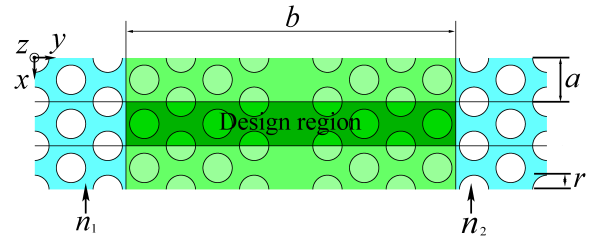


Fig. 2 Design model of low dispersion and slow light PCWG.



Fig. 3 Initial structure for optimization ($h=0$).

where δ is a step size for updating. For a large value of δ , C would not converge. On the other hand, for a small value of δ , it might need more iterations to achieve the convergence. In this paper, δ is set to be 0.01. This value δ is addressed in detail in the next section.

4. DESIGN EXAMPLE OF PHOTONIC CRYSTAL WAVEGUIDE

Here, in order to confirm the usefulness of the proposed optimization method, the low-dispersion and slow-light PCWGs with desired group index are designed. The structure of the PCWG is shown in Fig. 2. Considering the PC with the air hole radius of $r = 0.29a$, the design region width is set to be $b = 5\sqrt{3}a$. The refractive indices of the dielectric and air regions are $n_1 = 3.4$ and $n_2 = 1$, respectively. The dispersion property of TM mode is optimized. Let $N = 11$ in (20)–(22) and optimized region in the propagation constant is set to be $0.37 \leq \beta a / 2\pi \leq 0.48$. The low dispersion bandwidth is defined by $n'_g \pm 10\%$ [4]–[7], where n'_g is a central group index.

Figure 3 shows the initial structure used in this paper. We find that the air holes in the design region look like elliptical holes with the ellipticity of about 0.73 and the semi-major axis of about $0.28a$. This is because the structure in the design region is expressed using the finite number of terms of the Fourier series, that is, $w(x, y)$ in (9). In this paper, $w(x, y)$ is the Fourier series approximation for the ideal initial function $w_0(x, y)$ defined as

$$w_0(x, y) = \min_{i=1,2,\dots,N_h} \left\{ \sqrt{(x-x_{0,i})^2 + (y-y_{0,i})^2} / r - 1 \right\} \quad (26)$$

where $N_h (=12)$ is the number of air holes and $(x_{0,i}, y_{0,i})$ is the center coordinate of each air hole. The design region shown in Fig. 2 is exactly expressed if we can use $w_0(x, y)$ as $w(x, y)$ in (6), but we employ the initial structure for $N_x = 16$ and $N_y = 128$ in (9), as shown in Fig. 3. The dispersion properties of the ideal structure (Fig. 2) and the initial one (Fig. 3) are shown in Fig. 4, where the lattice constant is set to be 350 nm.

First, the desired group index n_g is set to be 100 and its optimized result is shown in Fig. 5. Figure 5(a) shows the convergence behavior of the objective function C . From this

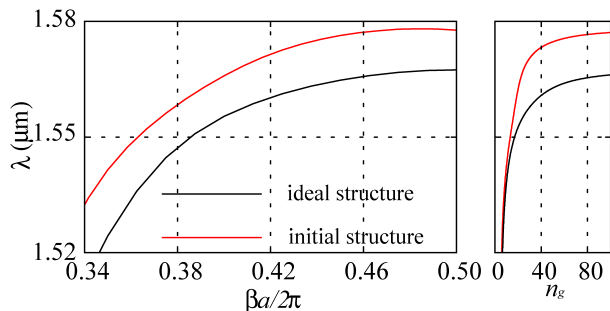


Fig. 4 Comparison of the initial structure and the ideal structure.

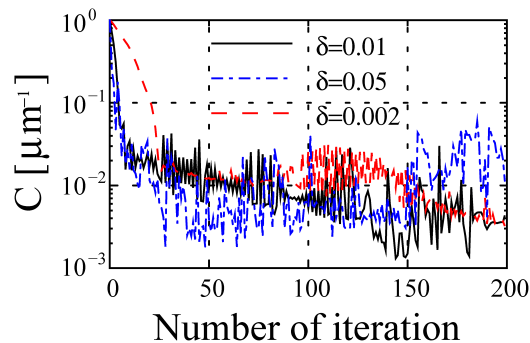
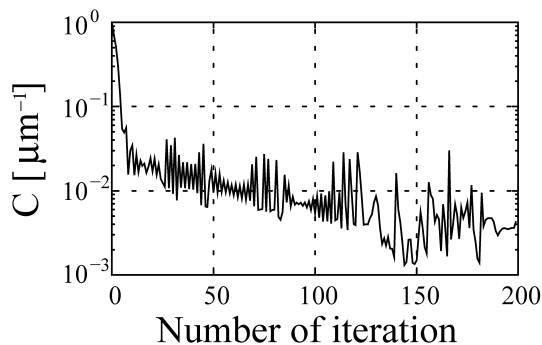


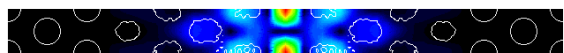
Fig. 6 Convergence of the objective function for each δ .



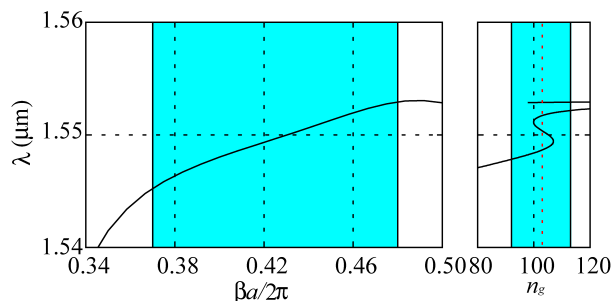
(a) Objective function



(b) Optimized structure



(c) Modal field ($\beta a/2\pi = 0.425$)



(d) Frequency dependency of propagation constant and group index

Fig. 5 Optimization of low dispersion and slow light PCWG ($n_g = 100$).

figure, we can see that C decreases oscillately. The optimum value of C is obtained at 144th iteration. Figure 5(b) and (c) show the optimized structure and modal field distribution at the normalized propagation constant $\beta a/2\pi = 0.425$. The dispersion curve and the frequency dependence of the group index are shown in Fig. 5(d). The obtained dispersion curve is in good agreement with the aimed dispersion curve except near the both edges of the considered propagation constant region. In the optimized structure, the group index of $n_g = 103$ and low-dispersion bandwidth of 4.3 nm are realized at

the central wavelength of 1.55 μm .

In this paper, δ is set to be 0.01. The convergence behavior of the objective function, C , may depend on the value of δ . The large δ accelerates the convergence, however the optimal solution may be jumped over. On the other hand, The smaller δ makes convergence slower. Figure 6 shows the convergence behavior of C when δ is set to be 0.002, 0.01, and 0.05. In this case, the minimum value of C is steadily obtained when δ is set to be 0.01.

Next, in order to confirm that this approach can be applicable to optimization for several waveguide dispersion properties, the desired group index n_g is set to be 50 and its optimized result is shown in Fig. 7. Figure 7(a) shows the convergence behavior of the objective function C . From this figure, we can see that the oscillation of C is suppressed compared to the case of $n_g = 100$. The optimum value of C is obtained at 176th iteration. Figure 7(b) and (c) show the optimized structure and modal field distribution at the normalized propagation constant $\beta a/2\pi = 0.425$. The dispersion curve and the frequency dependence of the group index are shown in Fig. 7(d). The obtained dispersion curve is also in good agreement with the aimed dispersion curve. In this optimization, the group index of $n_g = 50$ and low-dispersion bandwidth of 10.5 nm are realized at the central wavelength of 1.55 μm . The group index and operation bandwidth are in the trade-off relationship.

In the structural optimization, in general, the higher degree of design freedom can realize the better properties, however, the obtained structure tends to be complicated. In Fig. 5(b) and Fig. 7(b), the obtained PCWGs have complicated microscopic structure. We think these microscopic structures correspond to the gray area generated in the standard density method, i.e., the locally averaged refractive index around microscopic structures exhibits an intermediate value between the refractive indices of two usable materials. It may be possible to improve the dispersion property using more than two materials. However, in this problem, available materials are restricted to two materials. In section 6, we attempt to suppress these microscopic structures using structural filter.

5. TIME EVOLUTION OF OPTICAL PULSE

Next, in order to confirm the low-dispersion property of

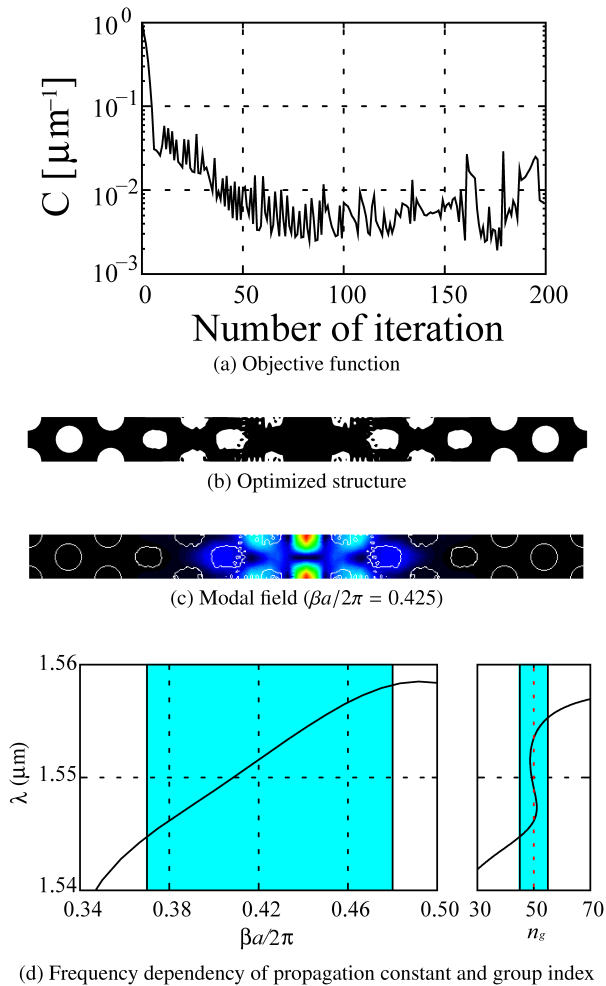


Fig. 7 Optimization of low dispersion and slow light PCWG ($n_g = 50$).

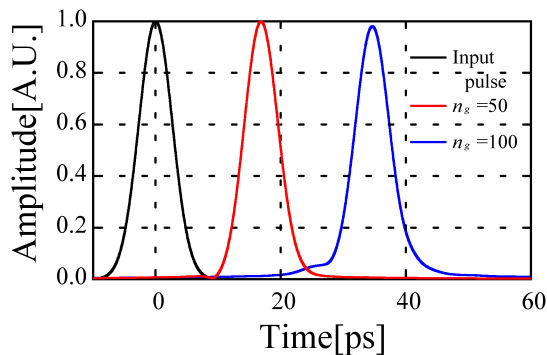


Fig. 8 Time evolution of Gaussian pulse.

the designed PCWGs, the time evolution of Gaussian pulse in them is analyzed. Figure 8 shows the input pulse and output pulse after $100 \mu\text{m}$ propagation. The time width of input pulse is assumed to be 2.7 ps , which corresponds to wavelength bandwidth of 3 nm . Although the pulse width is slightly broadened in the case of $n_g = 100$, the low-dispersion propagation is realized. The estimated group velocities of this analysis are $n_g = 50$ and $n_g = 100$, respectively.

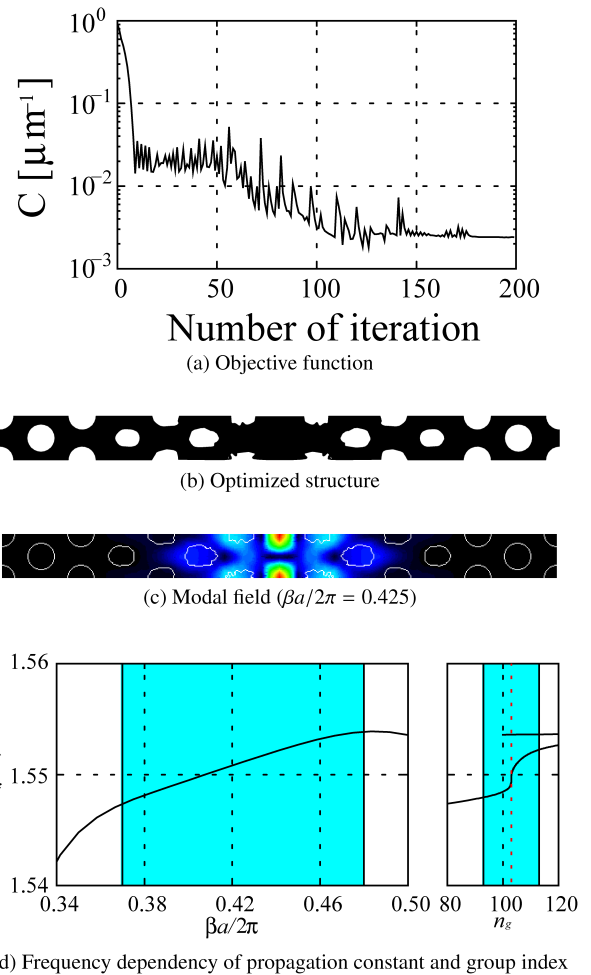


Fig. 9 Optimization of low dispersion and slow light PCWG ($n_g = 100$), where the Gaussian filter is used as a structural filter.

6. STRUCTURAL FILTER

Finally, in order to suppress the complicated structure, we introduce a structural filter. The complicated structure is the major issue of this optimization. This problem makes actual fabrication to be difficult, and the slight deviation of fabricated structure can degrade the wave-guiding property. The structural filters are used to smooth the current structure. Filter operation is expressed as a convolution integral:

$$w'(x, y) = \int_{-\infty}^{\infty} \int_{-\infty}^{\infty} w(\xi, \eta) g(x - \xi, y - \eta) d\xi d\eta \quad (27)$$

where w is a current structure, g is a filter function, and w' is a simplified structure. In this paper, w is actually given in the frequency domain. Therefore, the convolution integral can be rewritten as the simple product of W and G in the frequency domain.

$$W'(k_x, k_y) = W(k_x, k_y) G(k_x, k_y) \quad (28)$$

where $W(k_x, k_y)$ is the Fourier transform of $w(x, y)$ in (9), G is the Fourier transform of g . In this paper, we use the

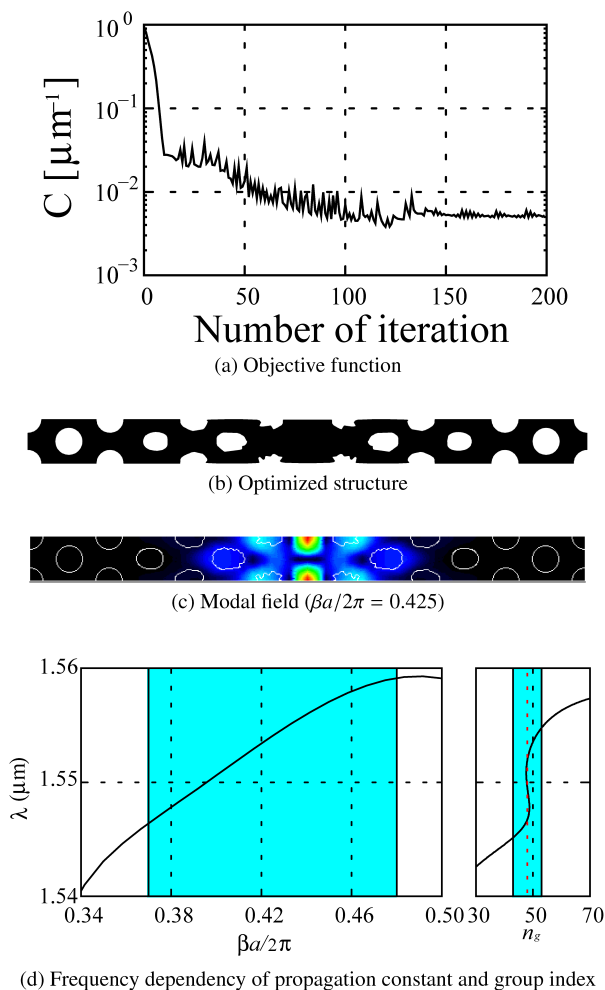


Fig. 10 Optimization of low dispersion and slow light PCWG ($n_g = 50$), where the Gaussian filter is used as a structural filter.

Gaussian filter defined by

$$G(k_x, k_y) = \frac{1}{2\pi\sigma^2} \exp\left(-\frac{k_x^2 + k_y^2}{2\sigma^2}\right), \quad (29)$$

where k_x and k_y is the frequency domain of x and y , σ is the effect of the Gaussian filter. In this paper, σ value is set to be $500 \text{ rad}/\mu\text{m}$. In this optimization, we use the initial structure of Fig. 3 and the objective function of (20)~(23). After updating the refractive index distribution, we introduce the structural filter.

First, the desired group index n_g is set to be 100 and its optimized result is shown in Fig. 9. Figure 9(a) shows the convergence behavior of the objective function C . The optimum value of C is obtained at 126th iteration. Figure 9(b) and (c) show the optimized structure and modal field distribution at the normalized propagation constant $\beta a/2\pi = 0.425$. Compared with the structure without using a smoothing filter shown in Fig. 5(b), the simpler optimized structure is obtained. The dispersion curve and the frequency dependence of the group index are shown in Fig. 9(d). The obtained dispersion curve is in good agreement with the aimed dispersion curve except near the both edges of the consid-

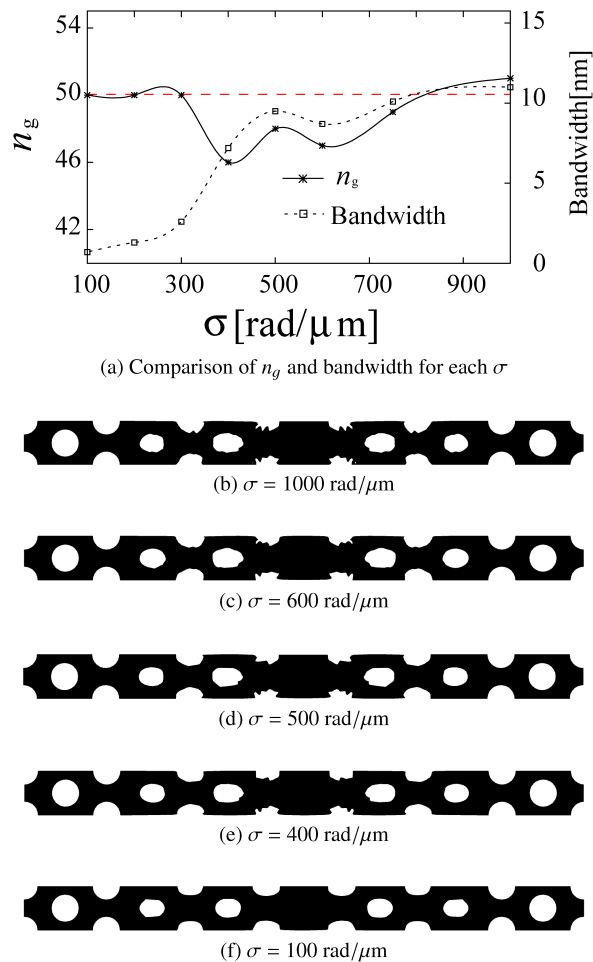


Fig. 11 Dependence of in the optimized structure and properties on σ .

ered propagation constant region. In the optimized structure, the group index of $n_g = 103$ and low-dispersion bandwidth of 4.3 nm are realized at the central wavelength of $1.55 \mu\text{m}$.

Next, the desired group index n_g is set to be 50 and its optimized result is shown in Fig. 10. Figure 10(a) shows the convergence behavior of the objective function C . The optimum value of C is obtained at 120th iteration. Figure 10(b) and (c) show the optimized structure and modal field distribution at the normalized propagation constant $\beta a/2\pi = 0.425$. The dispersion curve and the frequency dependence of the group index are shown in Fig. 10(d). The obtained dispersion curve is also in good agreement with the aimed dispersion curve. In this optimization, the group index of $n_g = 48$ and low-dispersion bandwidth of 9.5 nm are realized at the central wavelength of $1.55 \mu\text{m}$. This structure is simplified, compared with the structure without using a smoothing filter shown in Fig. 7(b). However, the bandwidth is slightly narrowed.

Finally, in order to verify the effect of the parameter σ in the filter function, we examine the dependence of the optimized property and structure on σ in detail. Figure 11 shows the optimized results for different σ values. When σ is set to be $1000 \text{ rad}/\mu\text{m}$, the smoothing effect does not seem to be sufficient. On the other hand, when σ is set to be

100 rad/ μm , the smoothing effect is too strong and the low dispersion property is not maintained. As a result, when σ is set to be 400 ~ 600 rad/ μm , the low dispersion property is realized in the relatively simple structure.

7. CONCLUSION

In this paper, we applied the function expansion based topology optimization method to the optimization problem of the waveguide dispersion and designed the low-dispersion and slow-light PCWGs. In order to realize two properties of low dispersion and desired group velocity, the objective function is expressed in the form of weighted sum of two terms and the priority of these terms is adaptively updated. In these problems, simply using the function expansion method, the complicated structure is sometimes obtained. Therefore, we introduced a structural filter to simplify the structure. At the next step, we will design novel high performance photonic devices by using this optimization method.

References

- [1] J. S. Jensen and O. Sigmund, "Systematic design of photonic crystal structures using topology optimization: Low-loss waveguide bends," *Appl. Phys. Lett.*, vol. 84, no. 12, pp. 2022–2024, Mar. 2004.
- [2] Y. Tsuji, K. Hirayama, T. Nomura, K. Sato, and S. Nishiwaki, "Design of optical circuit devices based on topology optimization," *IEEE Photon. Technol. Lett.*, vol. 18, no. 7, pp. 850–852, Apr. 2006.
- [3] Y. Tsuji and K. Hirayama, "Design of optical circuit devices using topology optimization method with function-expansion-based refractive index distribution," *IEEE Photon. Technol. Lett.*, vol. 20, no. 12, pp. 982–984, June 2008.
- [4] R. Matzen, J. S. Jensen, and O. Sigmund, "Systematic design of slow-light photonic waveguides," *J. Opt. Soc. Am. B*, vol. 28, no. 10, pp. 2374–2382, Oct. 2011.
- [5] F. Wang, J. S. Jensen, and O. Sigmund, "High-performance slow light photonic crystal waveguides with topology optimized or circular-hole based material layouts," *Photon. Nanostruct. Fundam. Appl.*, vol. 10, no. 4, pp. 378–388, Oct. 2012.
- [6] F. Wang, J. S. Jensen, and O. Sigmund, "Robust topology optimization of photonic crystal waveguides with tailored dispersion properties," *J. Opt. Soc. Am. B*, vol. 28, no. 3, pp. 387–397, Mar. 2011.
- [7] F. Wang, J. S. Jensen, J. Mork, and O. Sigmund, "Systematic design of loss-engineered slow-light waveguides," *J. Opt. Soc. Am. A*, vol. 29, no. 12, pp. 2657–2666, Dec. 2012.
- [8] T. P. White, L. C. Botten, C. M. de Sterke, K. B. Dossou, and R. C. McPhedran, "Efficient slow-light coupling in a photonic crystal waveguide without transition region," *Opt. Lett.*, vol. 33, no. 22, pp. 2644–2646, Nov. 2008.
- [9] J. Hou, D. Gao, H. Wu, R. Hao, and Z. Zhou, "Flat band slow light in symmetric line defect photonic crystal waveguides," *IEEE Photon. Technol. Lett.*, vol. 21, no. 20, pp. 1571–1573, Oct. 2009.
- [10] H. Goto, Y. Tsuji, T. Yasui, and K. Hirayama, "A study on function expansion based topology optimization method for dispersion property," 2013 International Symposium on Electromagnetic theory, no. 21PM1C-02, pp. 162–165, May 2013.
- [11] T. Baba, "Slow light in photonic crystals," *Nat. Photon.*, vol. 2, pp. 465–473, Aug. 2008.
- [12] Y. Tsuji and M. Koshiba, "Finite element method using port truncation by perfectly matched layer boundary conditions for optical waveguide discontinuity problems," *J. Lightw. Technol.*, vol. 20, no. 3, pp. 463–468, Mar. 2002.



Hiroyuki Goto received the B.S., degree in electrical and electronic engineering from Muroran Institute of Technology, Muroran, Japan, in 2012. He is presently working toward the M.S. degree in Information and Electronic Engineering from Muroran Institute of Technology. Mr. Goto is a student member of the Institute of Electronics, Information and Communication Engineers (IEICE).



Yasuhide Tsuji received the B.S., M.S., and Ph.D. degrees in electronic engineering from Hokkaido University, Sapporo, Japan, in 1991, 1993, and 1996, respectively. In 1996, he joined the Department of Applied Electronic Engineering, Hokkaido Institute of Technology, Sapporo, Japan. From 1997 to 2004, he was an Associate Professor of Electronics and Information Engineering at Hokkaido University. From 2004 to 2011, he was an Associate Professor of Electrical and Electronic Engineering at Kitami Institute of Technology, Kitami, Japan. Since 2011, he has been a Professor of Information and Electronic Engineering at Muroran Institute of Technology, Muroran, Japan. He has been interested in wave electronics. Dr. Tsuji is a member of the Institute of Electronics, Information and Communication Engineers (IEICE), the Japan Society of Applied Physics, the Optical Society of America (OSA), and IEEE. In 1997 and 1999, he was awarded the Excellent Paper Award from IEICE. In 2000, he has received the Third Millennium Medal from IEEE.

Since 2011, he has been a Professor of Information and Electronic Engineering at Muroran Institute of Technology, Muroran, Japan. He has been interested in wave electronics. Dr. Tsuji is a member of the Institute of Electronics, Information and Communication Engineers (IEICE), the Japan Society of Applied Physics, the Optical Society of America (OSA), and IEEE. In 1997 and 1999, he was awarded the Excellent Paper Award from IEICE. In 2000, he has received the Third Millennium Medal from IEEE.



Takashi Yasui received the B.S. degree in electronic engineering from Fukui University, Fukui, Japan, in 1997, and the M.S. and Ph.D. degrees in electronic engineering from Hokkaido University, Sapporo, Japan, in 1999 and 2001, respectively. From 1999 to 2002, he was a Research Fellow of the Japan Society for the Promotion of Science. In 2002, he joined Fujitsu Ltd., Chiba, Japan. From 2004 to 2011, he was an Assistant Professor of the Department of Electronic and Control Systems Engineering,

Shimane University, Matsue, Japan. Since 2011, he has been an Associate Professor of the Department of Electrical and Electronic Engineering, Kitami Institute of Technology, Kitami, Japan. He has been engaged in research on wave electronics. Dr. Yasui is a member of the Applied Computational Electromagnetics Society, the Optical Society of America, the Institute of Electronics, Information, and Communication Engineers of Japan, and the Magnetics Society of Japan.



Koichi Hirayama received the B.S., M.S., and Ph.D. degrees in electronic engineering from Hokkaido University, Sapporo, Japan, in 1984, 1986, and 1989, respectively. In 1989, he joined the Department of Electronic Engineering, Kushiro National College of Technology, Kushiro, Japan. In 1992, he became an Associate Professor of Electronic Engineering at Kitami Institute of Technology, Kitami, Japan, and in 2004 he became a Professor. He has been interested in the analysis and optimal design of

electromagnetic and optical waveguides. Dr. Hirayama is a member of the Japan Society of Applied Physics and a senior member of IEEE.